

# Molecular mechanism of the nuclear protein import cycle

Murray Stewart

**Abstract** | The nuclear import of proteins through nuclear pore complexes (NPCs) illustrates how a complex biological function can be generated by a spatially and temporally organized cycle of interactions between cargoes, carriers and the Ran GTPase. Recent work has given considerable insight into this process, especially about how interactions are coordinated and the basis for the molecular recognition that underlies the process. Although considerable progress has been made in identifying and characterizing the molecular interactions in the soluble phase that drive the nuclear protein import cycle, understanding the precise mechanism of translocation through NPCs remains a major challenge.

The spatial separation of transcription and translation provides eukaryotes with powerful mechanisms for controlling gene expression, but also necessitates selective transport between the nuclear and cytoplasmic compartments to maintain the distinctive composition of each. Consequently, the nuclear envelope is a crucial barrier across which both proteins and RNA have to be transported in a regulated manner. Moreover, in addition to bulk transfer of constitutive nuclear proteins such as histones following their synthesis in the cytoplasm, changes in gene expression generally require the controlled entry of key signalling molecules to the nucleus.

Macromolecules that are greater than ~40 kD are transported actively across the nuclear envelope through nuclear pore complexes (NPCs) using soluble transport factors or carrier molecules that cycle between the cytoplasm and nucleus<sup>1–11</sup>. NPCs (BOX 1) are huge macromolecular assemblies that perforate the nuclear envelope and form the conduit for the bidirectional exchange of molecules between the cytoplasm and nucleus through a central channel that has a limiting diameter of ~25–30 nm<sup>12</sup>. NPCs are constructed from multiple copies of ~30 different proteins collectively called nucleoporins<sup>13–15</sup>.

There are several nuclear transport pathways, each of which transports a specific range of macromolecules either into or out of the nucleus<sup>1–7</sup>. Most pathways use a homologous family of carrier molecules collectively called  $\beta$ -karyopherins, with import carriers called importins and export carriers called exportins. Many proteins are imported using importin- $\beta$  (often using importin- $\alpha$  as an adaptor), although some are imported using other importins, such as transportin; many proteins are exported using the export carrier

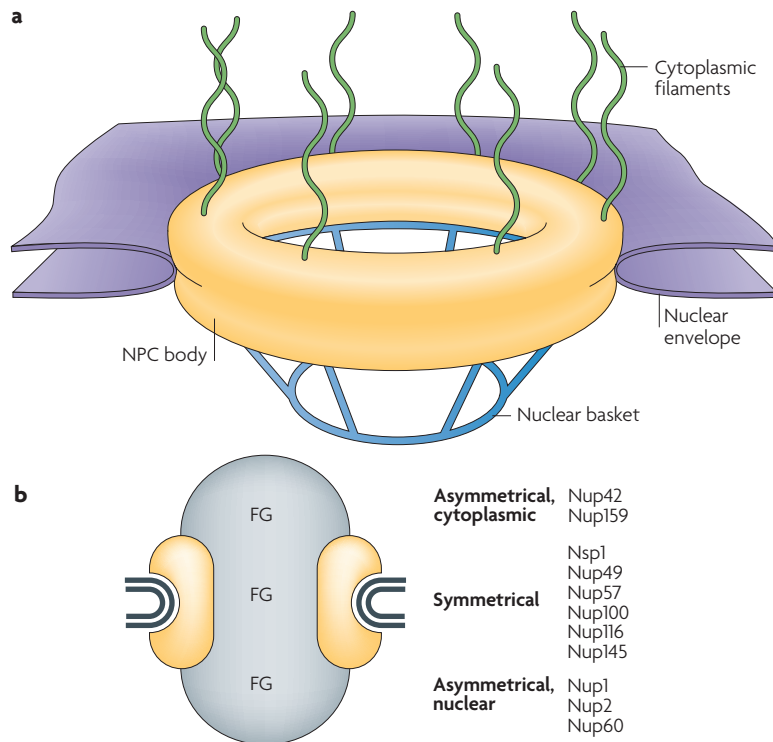
CRM1, whereas pre-microRNA and tRNA are exported by exportin-5 and exportin-t (all of which are importin- $\beta$  homologues). By contrast, mRNA export uses the NXF1: NXT1 heterodimer that is unrelated to karyopherins. The classic nuclear protein import pathway (FIG. 1) is the best characterized of these transport cycles, and all its components (TABLE 1) have been identified (reviewed in REFS 1–11). Here, the structures of these components and many of the complexes they form are reviewed in the context of recent work that has sought to establish how these proteins work together to generate function. Although a considerable number of components and interactions are required to generate nuclear transport, this system is still less complex than the systems that function in other central cellular processes, such as signalling, cell motility or vesicle transport. This, combined with the availability of structural information on most of the components and many of their complexes, makes the nuclear protein import cycle an attractive system in which to develop concepts that might serve as paradigms for how function is generated in more complex biological systems.

## Nuclear protein import pathways

There are different nuclear protein import pathways that use different carriers, but that share many common features and are based on a concerted series of protein: protein interactions by which cargoes are recognized in the cytoplasm, translocated through NPCs and released into the nucleus<sup>1–7</sup>. In each pathway, cargo proteins are targeted for nuclear import by short nuclear localization signal (NLS) sequence motifs. There are different NLS classes, each of which is recognized by the components of a different pathway. The classic nuclear protein import

MRC Laboratory of Molecular Biology, Hills Road, Cambridge CB2 2QH, UK.  
e-mail: ms@mrc-lmb.cam.ac.uk  
doi:10.1038/nrm2114  
Published online 7 February 2007

Box 1 | Nuclear pores



Nuclear pore complexes (NPCs) are huge supramolecular assemblies that span the outer and inner nuclear membranes and facilitate the bidirectional exchange of macromolecules between the cytoplasm and the nucleus. NPC morphology has been established by electron tomography<sup>86–91</sup> and is based on a doughnut-like central body, ~120 nm in diameter and 70 nm in width, that has 8-fold rotational symmetry. Fibres extend from the central body into both the cytoplasm and the nucleus, and, in the case of the nuclear fibres, these form a basket-like structure below the body of the NPC. The body of the NPC has a central ~25–30-nm diameter channel through which macromolecules are transported<sup>12</sup>, although the precise details of this feature are controversial<sup>86–91</sup>. Although this central channel is shown as empty in part **a** of the figure, it is thought to contain a high concentration of nuclear pore protein chains that have little regular structure. Three-dimensional reconstructions based on vitrified amphibian or yeast NPCs were initially thought to indicate the presence of a distinct cylindrical ‘transporter’ ~10 nm in diameter<sup>86,87</sup>, but more recent work has indicated that this feature instead represents material in transit<sup>88</sup>. NPCs are plastic structures<sup>86,91</sup> and appear to deform to accommodate the passage of large particles.

NPCs are constructed from multiple copies of ~30 different proteins, collectively called nucleoporins<sup>13–15,51</sup>. Most nucleoporins are located symmetrically and can be found on both the nuclear and cytoplasmic sides of NPCs, although a small subset are located asymmetrically and are found primarily on one side<sup>14,51</sup> because of where they are attached to the body of the NPC<sup>92</sup>. Biochemical fractionation of NPCs has shown that many nucleoporins associate with one another to form subcomplexes with a defined composition<sup>51</sup>. Nucleoporins seem to be constructed from a number of common protein folds, including coiled coils, WD propellers and  $\alpha$ -helical solenoids<sup>93</sup>. These folded domains are thought to be located primarily in the annular body of NPCs. In addition, many nucleoporins contain multiple copies of distinctive Phe-Gly (FG) sequence motifs<sup>13–15,51</sup> that appear to be located diffusely at either entrance to the pore<sup>5,14,89</sup> as well as in the central transport channel<sup>52</sup> (part **b** of the figure). The repeats in FG-nucleoporins have short hydrophobic cores containing Phe and Gly residues with sequences such as FXFG (in which X is a small residue such as Gly, Ala or Ser) or GLFG. These cores are separated by hydrophilic linkers of variable length and sequence.

pathway uses importin- $\beta$  as a carrier, transports a broad range of cargoes and has been studied in substantial biochemical, genetic, cell biological and structural detail. Although this pathway forms the focus of this

review, progress is also being made in our understanding of pathways that import ribosomal proteins<sup>16</sup>, histones<sup>17</sup> and heterogeneous nuclear ribonucleoproteins (hnRNPs) with M9 NLSs<sup>18</sup>, and that use different carriers and have NLSs that are distinct from those used in the classic pathway.

**The classic nuclear protein import cycle**

The classic nuclear protein import cycle (FIG. 1) generates transport rates of ~100–1,000 cargoes per minute per NPC<sup>19</sup> and is driven by a series of protein:protein interactions. Cargo proteins with a classic NLS are imported by the carrier importin- $\beta$ , which binds them through the adaptor protein importin- $\alpha$ <sup>1–11</sup>. Both importins are elongated molecules constructed from a tandem series of repeating sequence motifs (BOX 2, FIG. 2b and **Supplementary information S1, S2** (movies)). In the cytoplasm, cargo proteins that contain a classic NLS form an import complex with the importin- $\alpha$ : $\beta$  heterodimer, which facilitates movement through NPCs. In the nucleus, RanGTP binds to importin- $\beta$ , dissociating the import complex and releasing the cargo. Importin- $\beta$  complexed with RanGTP is recycled to the cytoplasm, whereas importin- $\alpha$  is exported complexed with the  $\beta$ -karyopherin CAS and RanGTP. Finally, cytoplasmic RanGAP (Ran GTPase activating protein) stimulates the Ran GTPase, generating RanGDP, which dissociates from the importins and thereby releases them for another import cycle.

The nuclear protein import cycle is based on a carefully choreographed series of interactions that must be controlled precisely both spatially and temporally. Molecular recognition is crucial to the cycle, both in terms of carriers recognizing their cargoes and also in distinguishing between the nuclear and cytoplasmic compartments. Interactions between cargoes and carriers are orchestrated by the nucleotide state of Ran, which cycles between GTP- and GDP-bound states (FIG. 1b). The Ran nucleotide state is controlled by its guanine nucleotide-exchange factor (RanGEF), which catalyses recharging of RanGDP with GTP, and RanGAP, which stimulates GTP hydrolysis. RanGEF is nuclear and RanGAP is cytoplasmic, and so nuclear Ran is in the GTP-bound state, whereas cytoplasmic Ran is GDP bound. RanGTP is exported from the nucleus bound to  $\beta$ -karyopherin carriers and, after RanGAP-mediated GTP hydrolysis, cytoplasmic RanGDP is transported to the nucleus by its specific carrier, nuclear transport factor-2 (NTF2)<sup>20,21</sup>, for recharging with GTP.

The conformation of key structural loops in Ran (the switch I and II loops) changes markedly with nucleotide state (BOX 2 and **Supplementary information S3** (movie)). This structural change determines the way in which importin- $\beta$  family transport factors interact with cargoes, and so ultimately, the Ran GTPase provides the energy for nuclear transport.

The nuclear protein import cycle can be conveniently divided into four steps: assembly of the cargo:carrier import complex in the cytoplasm; translocation through NPCs; import-complex disassembly in the nucleus; and importin recycling.

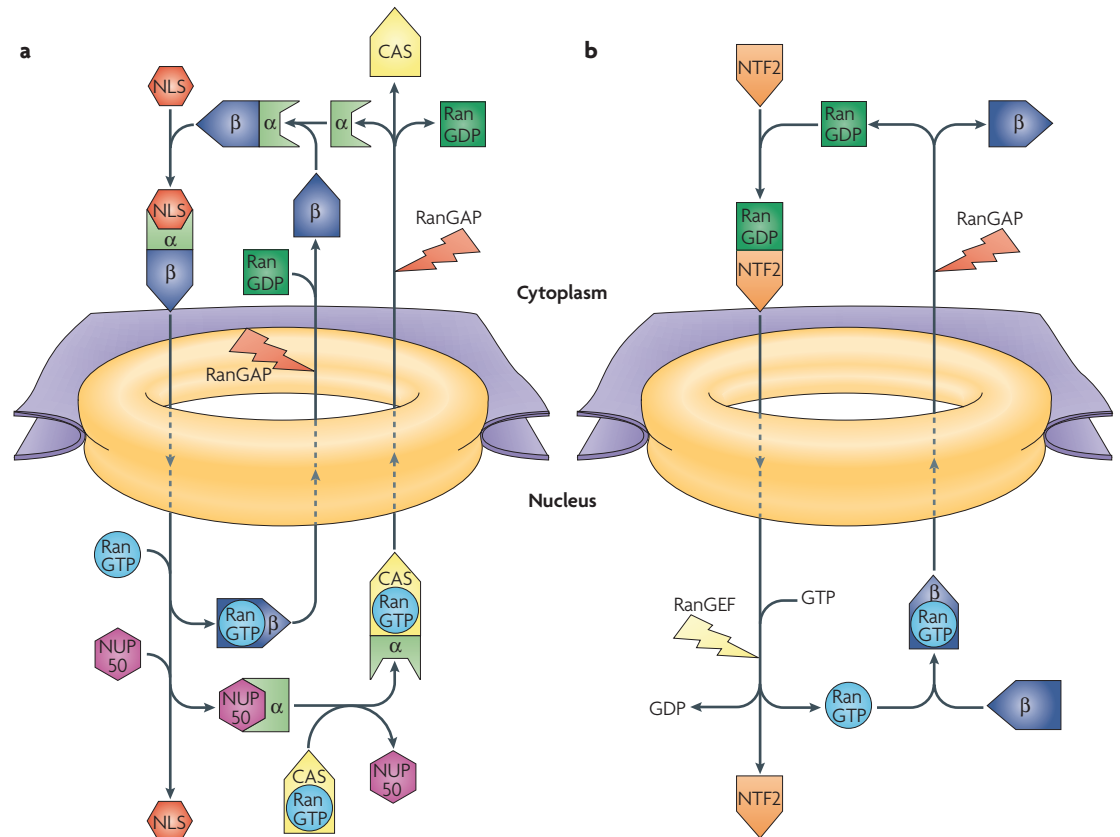


**Figure 1 | Overview of nuclear protein import. a** | An import complex is formed in the cytoplasm between cargoes bearing nuclear localization signals (NLSs), importin- $\alpha$  and importin- $\beta$ . After passing through the nuclear pore complex (NPCs), the binding of RanGTP to importin- $\beta$  dissociates importin- $\beta$  from importin- $\alpha$ . The NLS-containing cargo is then displaced from importin- $\alpha$  and the importin- $\alpha$  is recycled to the cytoplasm by its nuclear export factor, CAS, complexed with RanGTP. In the cytoplasm, RanGAP stimulates GTP hydrolysis, releasing the importins for another import cycle. Nucleoporins such as NUP50 catalyse cargo dissociation and function as molecular ratchets to prevent futile cycles. **b** | Ran also cycles between the nucleus and cytoplasm and, because the Ran guanine nucleotide-exchange factor (RanGEF) is nuclear and Ran GTPase activating protein (RanGAP) is cytoplasmic, this cycle is associated with changes in the nucleotide state. Therefore, cytoplasmic RanGDP is imported into the nucleus by nuclear transport factor-2 (NTF2), where RanGEF catalyses nucleotide exchange and generates RanGTP. RanGTP then binds to transport factors, such as importin- $\beta$  and CAS, and is exported to the cytoplasm, where RanGAP stimulates GTP hydrolysis. The structure of two loops in Ran (the switch I and II loops) changes markedly with nucleotide state (see BOX 2 and [Supplementary information S3](#) (movie)) and this change enables Ran to orchestrate the binding and release of its partners during the import cycle.

**Coiled coil**

A protein fold in which two  $\alpha$ -helices coil around one another.

**WD propeller**

A protein fold formed by a series of repeating WD sequence motifs that structurally resemble the blades of a propeller.

**$\alpha$ -helical solenoid**

A protein fold formed by successive repeats, each of which contains a number of  $\alpha$ -helices that form a loop that is like a coil of a spring or solenoid.

**Adaptor proteins**

Proteins that augment cellular responses by recruiting other proteins to a complex. They usually contain several protein: protein interaction domains.

**Scanning Ala mutagenesis**

A technique in which successive residues in a region of a sequence of a protein are mutated to Ala to define those that influence an activity, such as binding to another protein.

**Step 1: import-complex assembly**

Classic NLSs contain one or two clusters of basic residues (FIG. 2a). Monopartite NLSs, exemplified by the SV40 large-T antigen, have a single cluster of 4–5 basic residues, whereas bipartite NLSs, such as that of nucleoplasmin, have a second basic cluster located ~10–12 residues downstream of the first cluster (FIG. 2a). Molecular recognition of NLSs is crucial for the formation of the import complex and is mediated by specific sites on importin- $\alpha$ <sup>22–24</sup>. Importin- $\alpha$  is constructed from a tandem series of Armadillo (ARM) repeats that generates a banana-shaped molecule (FIG. 2 and [Supplementary information S1](#) (movie)), and the NLS-binding sites are formed from an array of Trp, Asn and acidic residues that are located in a groove on the inner concave surface (FIG. 2b–d). The primary binding site for monopartite NLSs spans ARM repeats 1–4 (the major site), and a secondary site (the minor site) spans

ARM repeats 6–8 (REFS 22–24). With bipartite NLSs, the larger basic cluster occupies the major site, and the smaller basic cluster occupies the minor site. Residues in the monopartite NLS and in the larger cluster in bipartite NLSs are referred to as P1–P6, whereas those in the second site in bipartite NLSs are referred to as P'1–P'4 (FIG. 2c,d). The basic side chains of the NLSs make a series of specific interactions with key residues along the inner surface of importin- $\alpha$  (FIG. 2c,d)<sup>22–24</sup>. Scanning Ala mutagenesis indicates that the Lys residue at position P2 is particularly important for this interaction, although positions P3 and P5 are also important<sup>25,26</sup>. Generally, the NLS accommodates to the binding site and so is usually present as an unstructured surface loop in the cargo protein, although sometimes the NLS is formed from disparate regions of a protein<sup>27</sup>. Moreover, a few cargo proteins bind directly to importin- $\beta$ <sup>28,29</sup>, rather than through importin- $\alpha$ .

Table 1 | Soluble components of the nuclear protein import cycle

Component	Other names	Function
Importin-β	Kap95*, Kap-β1, karyopherin-β	Transport factor that carries cargoes through NPCs
Importin-α	Kap60*, Srp1*, karyopherin-α	Adaptor that links NLS-containing cargoes to importin-β
CAS	Cse1*	Nuclear export factor for importin-α
Ran	Gsp1*	Ras-family GTPase that coordinates interactions
RanGAP	Ran1*	Ran GTPase activating protein
RanGEF	RCC1, Prp20*	Ran guanine nucleotide-exchange factor
NTF2	p10	Nuclear import factor for RanGDP
RanBP1	Yrb1*	Accessory protein that assists the dissociation of RanGDP from importin-β in the cytoplasm

\**Saccharomyces cerevisiae*. NLS, nuclear localization signal; NPC, nuclear pore complex; NTF2, nuclear transport factor-2.

The N terminus of importin-α binds to importin-β through a domain known as the importin-β binding (IBB) domain<sup>30,31</sup> (BOX 2 and [Supplementary information S2](#) (movie)), which also facilitates cargo release in the nucleus<sup>32</sup> (FIG. 2e). The IBB domain contains a cluster of basic residues that is similar to an NLS and can bind to the NLS-binding sites<sup>32,33</sup> (FIG. 2e). Therefore, in addition to connecting importin-α to importin-β, the IBB domain has an autoinhibitory role<sup>32</sup> so that, when it is not bound to importin-β, it competes with NLSs for binding to importin-α and so contributes to cargo release (see below). Consistent with this hypothesis, the affinity of importin-α constructs that lack the IBB-domain (ΔIBB-importin-α) for NLSs is substantially higher than that of the full-length protein<sup>34–36</sup>. However, importin-α usually has higher affinity for NLSs than for the IBB domain and so cargoes will still bind to full-length importin-α, but with lower affinity than observed for the ΔIBB construct<sup>36</sup>. When the IBB domain binds to importin-β, it can no longer compete with NLSs for binding to importin-α. Therefore, in the cytoplasm, NLS-containing cargoes probably bind primarily to the importin-α:β complex rather than to importin-α alone. Usually, NLSs have ~10-nM affinity for either ΔIBB-importin-α or for the importin-α:β complex<sup>34–36</sup>, and the rate of nuclear import correlates with the strength of binding to importin-α<sup>37</sup>.

The way in which importin-α recognizes NLSs is different to the way in which non-classic NLSs are recognized directly by other β-karyopherins. For example, importin-β binds sterol-response-element-binding protein-2 (SREBP2) by using the extended α-helices of HEAT repeats 8 and 17 like chopsticks<sup>28</sup>, whereas recent structural work on transportin has shown how it binds to M9 NLSs that have a central basic or hydrophobic motif followed by a distinctive R/H/KX<sub>(2–5)</sub>PY consensus sequence<sup>18</sup>.

### Step 2: translocation through NPCs

Macromolecules of  $M_r > 40$  kD are excluded from NPCs, and only those bound to carriers can move through the central transport channel, whereas smaller molecules can simply diffuse through NPCs. However, both the

mechanism by which cargo:carrier complexes are translocated through NPCs and the mechanism by which other molecules are excluded remain controversial. Single-molecule-fluorescence studies<sup>38</sup> indicate that movement of cargo:carrier complexes through NPCs is bidirectional and rapid, resembling a random walk, and overall it seems to be a first-order process in which the rate is limited by cargo exit. Therefore, directionality of transport is not imposed by the pore itself, but instead by RanGTP-induced dissociation of the cargo:carrier import complex in the nucleus. Translocation of cargo:carrier complexes is faster than translocation of carriers alone, and there seem to be multiple parallel pathways of transport<sup>39</sup>. Moreover, both import time and transport efficiency seem to depend on importin-β concentration<sup>40</sup>. Which molecules are transported through the nuclear pores is determined primarily by the carriers, each of which binds a specific range of cargoes (although there is sometimes a level of promiscuity; some cargoes can be transported by more than one carrier)<sup>1–11</sup>.

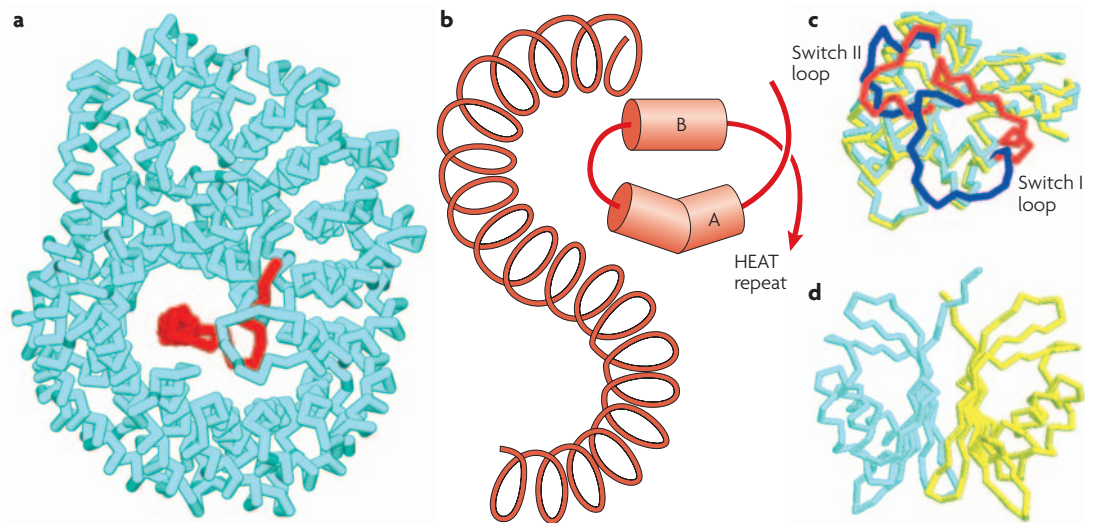
**FG-nucleoporins.** A subset of NPC proteins that contain distinctive tandem Phe-Gly (FG) sequence repeats<sup>13–15</sup> (FG-nucleoporins) are thought to be important for mediating both the movement of cargo:carrier complexes through NPCs and for excluding other macromolecules from the central transport channel of NPCs<sup>41–51</sup>. FG-nucleoporins typically contain ~20–30 of these repeats<sup>13–15,50,51</sup>, and electron-microscopy studies<sup>14,52</sup> indicate that the repeats are clustered around the nuclear and cytoplasmic faces of NPCs as well as in the central transport channel (BOX 1). There are probably ~3,500 FG repeats per NPC<sup>13–15,41,50,51</sup>. The FG-repeat regions of nucleoporins appear to have little ordered structure<sup>42,53,54</sup> and are sufficiently flexible to be able to move through the NPC from one side to the other<sup>5,55</sup>.

The Phe side chains of the hydrophobic FG-repeat cores bind to shallow hydrophobic cavities on the surface of carriers<sup>41–46,56</sup>. The interaction is weak (usually of the order of μM affinity) and so is sufficiently transient to enable rapid transport of cargo:carrier complexes (a high affinity would imply slow off-rates<sup>41</sup>). Engineered mutants with attenuated affinity for FG-nucleoporin cores have shown that this interaction is necessary for the nuclear import of both importin-β and Ran<sup>41–45,57</sup>. In addition to an interaction between carriers and the FG-repeat cores, there might also be contributions from the linkers between the cores. For example, different regions of the GLFG-repeat region of *Saccharomyces cerevisiae* nucleoporin Nup100 that contain the same number of GLFG cores have different affinities for importin-β<sup>49</sup>. Structural studies have also shown how a linker between FG cores can contribute to the interaction between importin-β and the *S. cerevisiae* nucleoporin Nup1 (REF. 56). Consequently, although binding to FG cores is central to the interaction between importin-β and nucleoporins, the linker regions might modulate the strength of the interaction. Moreover, the avidity of each FG-nucleoporin for carriers depends on the number of FG repeats, and so there is considerable variation in the apparent affinity of isolated nucleoporins for

#### Random walk

The path followed by taking successive steps, each in a random direction relative to the previous step.

## Box 2 | Structure of the key molecules in the nuclear protein import cycle



Importin- $\beta$ <sup>56,74,75</sup> (which is shown complexed with the importin- $\beta$  binding (IBB) domain of importin- $\alpha$  (red) in part a of the figure and in [Supplementary information S2](#) (movie)) is constructed from 19 HEAT repeats, each of which is made up of two  $\alpha$ -helices (A and B, part b). These HEAT repeats stack together to generate an elongated helicoidal molecule that is formed from two C-shaped arches<sup>56,74,75</sup>. The export carrier of importin- $\alpha$ , known as CAS (see [Supplementary information S7, S8](#) (movies)) has a similar helicoidal configuration based on 19 HEAT repeats<sup>33,79</sup>. The two  $\alpha$ -helices (cylinders A and B) from which HEAT repeats are constructed function like the coils of a spring (part b) and impart considerable flexibility to importin- $\beta$  and CAS that is crucial for orchestrating their binding and release of partners. Ran (part c and [Supplementary information S3](#) (movie)) has the Ras-family GTPase fold. Most of the Ran structure shows only marginal changes in conformation between the GTP- (cyan) and GDP-bound (yellow) states, but two loops (the switch I and switch II loops) change conformation markedly depending on whether GDP (red) or GTP (blue) is bound<sup>33,73,74,94,95</sup>. The C terminus also changes with nucleotide state, although the conformation taken up in the GTP-bound state appears to vary depending on the partner to which Ran is bound. NTF2 (REF. 96) (part d and [Supplementary information S11](#) (movie)) is constructed from two chains (cyan and yellow) and is the nuclear transport factor for RanGDP<sup>17,18</sup>. NTF2 (REF. 96) is a dimer in which there is a hydrophobic cavity that binds RanGDP<sup>95</sup> ([Supplementary information S12](#) (movie)) and also a hydrophobic patch formed by residues from each chain at the opposite end of the molecule, which binds nucleoporin FXFG repeats<sup>41,44,95,96</sup>. Ran guanine nucleotide-exchange factor (RanGEF) has a 7-bladed propeller structure<sup>97</sup> (see [Supplementary information S13](#) (movie)), and, by stabilizing the nucleotide-free state of Ran, increases the rate of nucleotide exchange by  $\sim 10^5$ . Ran GTPase activating protein (RanGAP)<sup>98</sup> is based on a leucine-rich repeat (LLR) fold (see [Supplementary information S14](#) (movie)) and increases the Ran GTPase activity by  $\sim 10^5$  (REF. 99). Movies showing the structure of each molecule rotating can be accessed online ([Supplementary information S1–S14](#) (movies)). Part b is reproduced with permission from REF. 81 © (2003) American Association for the Advancement of Science.

carriers *in vitro*, although this might not apply *in vivo*, as different nucleoporin chains probably intermingle at the NPC. In the case of the importin- $\alpha$ : $\beta$  import complex, the apparent affinity of isolated nucleoporins for the complex increases progressively moving from the cytoplasmic to the nuclear face of the NPC, and this gradient has been proposed to function as a driving force for nuclear import<sup>58,59</sup>. However, because the asymmetrically distributed nucleoporins are not essential<sup>50,60</sup> and, moreover, reversing the RanGTP concentration gradient<sup>61</sup> can reverse transport, it seems unlikely that the nucleoporin-affinity gradient is important in powering nuclear protein import, although it might have a catalytic role<sup>34,35,56</sup>.

The permeability of NPCs is surprisingly insensitive to the deletion of the FG repeats from many nucleoporins. A systematic deletion of the FG-repeat regions of 11 yeast nucleoporins in various combinations showed that the FG domains of asymmetrically located nucleoporins were not essential *in vivo*<sup>50</sup>. Deletion of the repeats from all 5 asymmetrical FG-nucleoporins or

combinatorial deletions of symmetrical nucleoporin FG repeats produced only a 3–4-fold decrease in the rate of import of an NLS-containing cargo, although specific combinations of symmetrically organized nucleoporins were essential<sup>50</sup>. Over half of the total mass of FG repeats could be deleted without loss of viability or loss of the normal barrier function of NPCs and, moreover, the influence of deletions was different on different import pathways. Remarkably, there was no correlation between the mass of FG repeats deleted and viability — deletion of the GLFG repeats of Nup100 and Nup116 was lethal, although they represent only a small fraction of the total FG-repeat mass<sup>50</sup>. Crucially, these studies showed that, although all the FG-nucleoporins contained similar repeating sequence motifs, not all FG repeats are equivalent. Therefore, in addition to facilitating the passage of cargo:carrier complexes through NPCs, particular FG-nucleoporins, or perhaps specific repeats within them, seem to have additional functions that remain to be defined precisely.

**Models of selective transport.** The concentration of FG repeats in the NPC transport channel is high, probably on the order of 10 mM or ~200–300 mg per ml<sup>41</sup> and this, combined with their native unfolded conformation<sup>53,54</sup>,

might obstruct the passage of macromolecules. Therefore, it has been proposed that the molecular crowding caused by the high concentration of FG repeats might exclude large macromolecules entropically<sup>14,62,63</sup>. This exclusion

**a Typical NLSs**

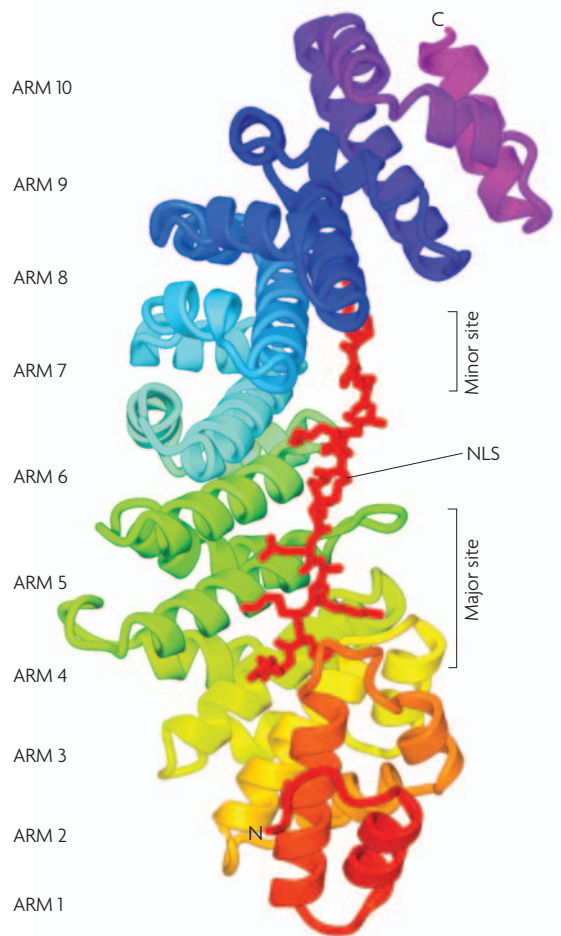
Monopartite NLS (SV40 large-T antigen)



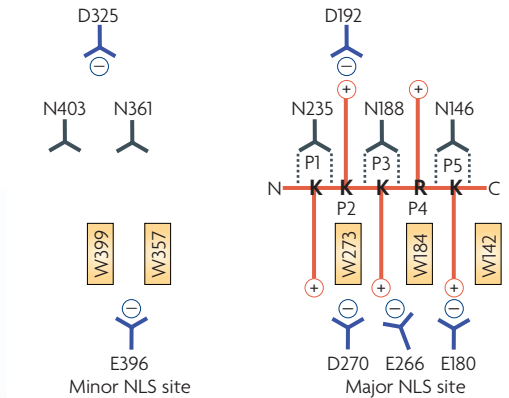
Bipartite NLS (nucleoplasmin)



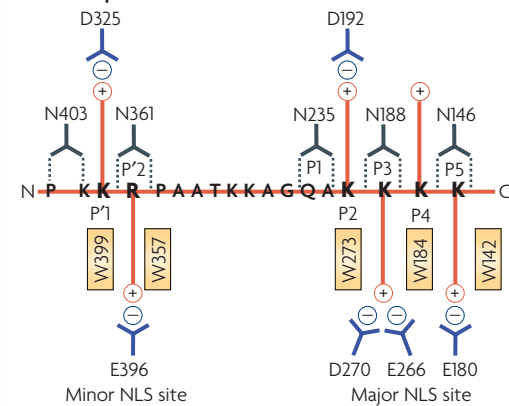
**b**



**c SV40 large-T antigen NLS**



**d Nucleoplasmin NLS**



**e**

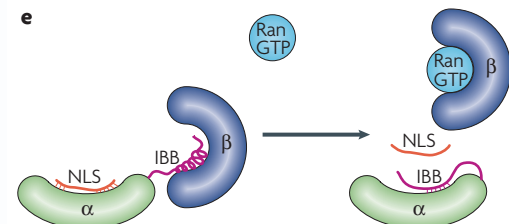


**Figure 2 | Formation of the importin- $\alpha$ :cargo complex in the cytoplasm.** **a** | Cargoes for nuclear import have nuclear localization signals (NLSs). The karyopherin importin- $\alpha$  recognizes classic NLSs based on one (monopartite) or two (bipartite) clusters of basic residues that are shown in red. **b** | Structure of the nucleoplasmin NLS (red) bound to importin- $\alpha$ <sup>23</sup>. The 10 different Armadillo (ARM) repeats of importin- $\alpha$  are shown in different colours. The NLS-binding sites are located in a groove on the inner surface of importin- $\alpha$ : the major binding site spans ARM repeats 1–4, whereas the minor site spans ARM repeats 6–8. **c** | Schematic illustration of the interactions between the SV40 large-T antigen NLS (shown in red with each residue identified in black one-letter code) and importin- $\alpha$  that are crucial for molecular recognition<sup>23</sup>. The key residues in the binding site are referred to as P1–P5. The hydrophobic portions of the basic side chains of residues in sites P3 and P5 are sandwiched between the indole side chains of residues W273, W184 and W142 of importin- $\alpha$  (yellow rectangles), whereas their charged (+) nitrogens form salt bridges with acidic (blue) residues D270, E266 and E180 (–) of importin- $\alpha$ . Lys P2 is neutralized by D192 (REFS 21–24). In addition, hydrogen bonds (dotted lines) are formed between Asp residues (N235, N188 and N146) and the NLS main-chain amides. **d** | Similar schematic showing the interactions between the nucleoplasmin NLS (shown in red) and importin- $\alpha$ , for which, in addition to the interactions at the major site (P2–P5), there are also similar interactions at the minor site (P'1–P'2). **e** | Schematic illustration of the autoinhibitory role of the importin- $\beta$  binding (IBB) domain. In the import complex, the IBB is bound to importin- $\beta$  (blue), but when released by RanGTP (cyan), it can compete with NLSs for binding to the importin- $\alpha$  ARM domain (green), leading to cargo release<sup>32</sup>.

would come about because, at high concentrations, the FG-repeat polypeptide chains get in each other's way and this crowding limits the number of conformations each can take up. At high concentrations, the chains cannot adopt the random-walk path that is expected for an unfolded polypeptide chain<sup>64</sup> and they become more extended, like the bristles in a brush<sup>65</sup>. These arrangements of chains, in which movement is restricted, are more ordered and have lower entropy (and therefore higher free energy) than free chains in solution, and so resist the increased crowding that results from introducing another macromolecular chain. Recent *in vitro* experiments support the hypothesis that high concentrations of FG repeats can form molecular brushes<sup>62</sup>.

Alternatively, it has been proposed that the FG-nucleoporin repeats form a sieve-like gel through interactions between hydrophobic FG cores<sup>16,48,66</sup>. The diffusion of particles in a crosslinked gel depends crucially on the gel's pore size<sup>67</sup>: particles above the pore size cannot diffuse, whereas the diffusion rate of particles below the pore size is only slightly reduced. In this model, the diffusion limit of ~40 kD for NPCs would be a consequence of the pore size of the FG-nucleoporin gel being of this order. Recent work has shown that the FG-repeat region of *S. cerevisiae* nucleoporin Nsp1 can indeed form a three-dimensional network with hydrogel-like properties and that gelation depends crucially on the Phe residues of the repeat cores<sup>66</sup>.

In both the molecular crowding and hydrogel/sieve models, cargo:carrier complexes are proposed to be able to overcome the barrier produced by the FG-nucleoporins through their interactions with FG-repeat cores. The molecular crowding model proposes that the enthalpy of binding compensates for the entropic penalty of penetrating the closely packed nucleoporin chains<sup>14,63</sup>, whereas the hydrogel/sieve model proposes that the interaction with the carrier locally disrupts interactions between FG-repeat cores that generate the gel and so transiently opens adjacent meshes in the gel<sup>66</sup>. Because both models rely on the high concentration of nucleoporins and their interaction with carriers, it is difficult to distinguish between them experimentally. Both models for exclusion require high concentrations of FG repeats and so might not be easily reconciled with the observation that nuclear transport and viability are preserved in *S. cerevisiae* in which over 50% of the nucleoporin FG repeats have been deleted<sup>50</sup>. Instead, specific FG-nucleoporin repeats in defined locations might be more important in limiting permeability<sup>50</sup>.

It has also been proposed<sup>10,34,35,56,68</sup> that FG repeats could influence transport rates by concentrating soluble components of the classic nuclear protein import machinery (such as importin- $\alpha$ , importin- $\beta$  and Ran) at NPCs. Indeed, this concentration is commonly seen in fluorescence-microscopy studies. Because the distance between NPCs on the nuclear envelope is usually on the order of  $\mu\text{m}$ <sup>69</sup>, the chances of molecules in the cytoplasm colliding with an NPC are small and the selective concentration of appropriate macromolecules in the vicinity of NPCs would facilitate their colliding with the entrance to the pore. FG-repeat-containing

fibrils that extend several  $\mu\text{m}$  into the cytoplasm might also facilitate transport by guiding bound cargo:carrier complexes to the transport channel<sup>10,70</sup>, similar to the way the tentacles of a sea anemone help to concentrate food at its mouth. However, such a mechanism is unlikely to account completely for selectivity because the cytoplasmic filaments are not absolutely required for nuclear protein import<sup>71</sup>. Naturally, these mechanisms are not mutually exclusive and might all contribute to selectivity.

Several mechanisms have been proposed to account for how cargo:carrier complexes move through NPCs (reviewed in REF. 51). Hydrophobic interactions between the carrier proteins and FG-repeat cores are clearly important, and engineered transport factors with reduced affinity for FG-nucleoporins fail to support nuclear transport<sup>41–45</sup>. The interaction between many carriers and FG-nucleoporin cores seems to generally be promiscuous. Moreover, most FG-repeat regions seem to be localized diffusely in the NPC transport channel and so nonspecific interactions between transport factors and different FG-repeat cores probably facilitate much of the passage of cargo:carrier complexes through NPCs. However, studies discussed above<sup>50</sup> in which the FG repeats of individual nucleoporins were deleted indicated that, in addition to these promiscuous interactions, there are also specific interactions that are crucial for transport, although the precise contribution made by each remains to be established.

The molecular mechanism by which the FG-nucleoporin repeats facilitate the movement of cargo:carrier complexes through NPCs is controversial. It has been proposed that cargo:carrier complexes jump from one FG repeat to the next, which has been likened to using the repeats like stepping stones<sup>72</sup> or like sliding over oily spaghetti<sup>2</sup>. Alternatively, FG-nucleoporins might provide a selective phase in which only the transport factors are soluble<sup>16,48</sup>.

### Step 3: import-complex disassembly

Nuclear RanGTP dissociates the cargo:carrier import complex and therefore imposes directionality on the transport process. The rapid diffusion of the cargo:carrier complex back and forth in the NPC transport channel<sup>40</sup> maintains a rapid equilibrium across the NPC, and so it follows from Le Chatelier's principle that removal of the complex from the nuclear side of the NPC by its dissociation by RanGTP will result in a net flow of cargo:carrier complex from the cytoplasm to the nucleus to restore the equilibrium. At a molecular scale, this is equivalent to saying that although thermal energy (Brownian motion) allows cargo bound to its carrier to diffuse rapidly in either direction through the NPC channel, the cargo cannot return to the cytoplasm after it has dissociated from its carrier in the nucleus. Ultimately, therefore, the energy of RanGTP hydrolysis rectifies the Brownian motion of the cargo:carrier complex, and so generates a thermal ratchet that imposes directionality on the transport by dissociating the import complex.

#### Entropy

The component of free energy due to the disorder or randomness of the system. Increases in entropy (disorder) lower the free energy, whereas increases in order (lower entropy) increase energy.

#### Enthalpy

The heat component of free energy that, in biological systems, is derived primarily from chemical bonds.

#### Le Chatelier's principle

Le Chatelier's principle states that if a dynamic equilibrium is disturbed by changing conditions, the position of equilibrium moves to counteract the change.

#### Thermal ratchet

A molecular mechanism by which the thermal (Brownian) motion of a particle is biased (or rectified) so that there is net movement in a particular direction. A thermal ratchet requires an input of energy in order not to violate the second law of thermodynamics.

## Helicoidal pitch

The distance along the axis of a helix corresponding to a rotation of 360°.

**Dissociation of the importin- $\alpha$ : $\beta$  complex.** The binding of RanGTP to importin- $\beta$  dissociates the importin- $\alpha$ : $\beta$  complex, leading to release of the cargo. There is only limited overlap between the RanGTP and the IBB-domain-binding sites on importin- $\beta$ , and so RanGTP releases the

importin- $\alpha$  IBB domain primarily by inducing a conformational change in importin- $\beta$ , rather than by competition (FIG. 3c). This conformational change increases the helicoidal pitch of importin- $\beta$ , thereby releasing the IBB domain mainly by an allosteric mechanism<sup>73,74</sup>.

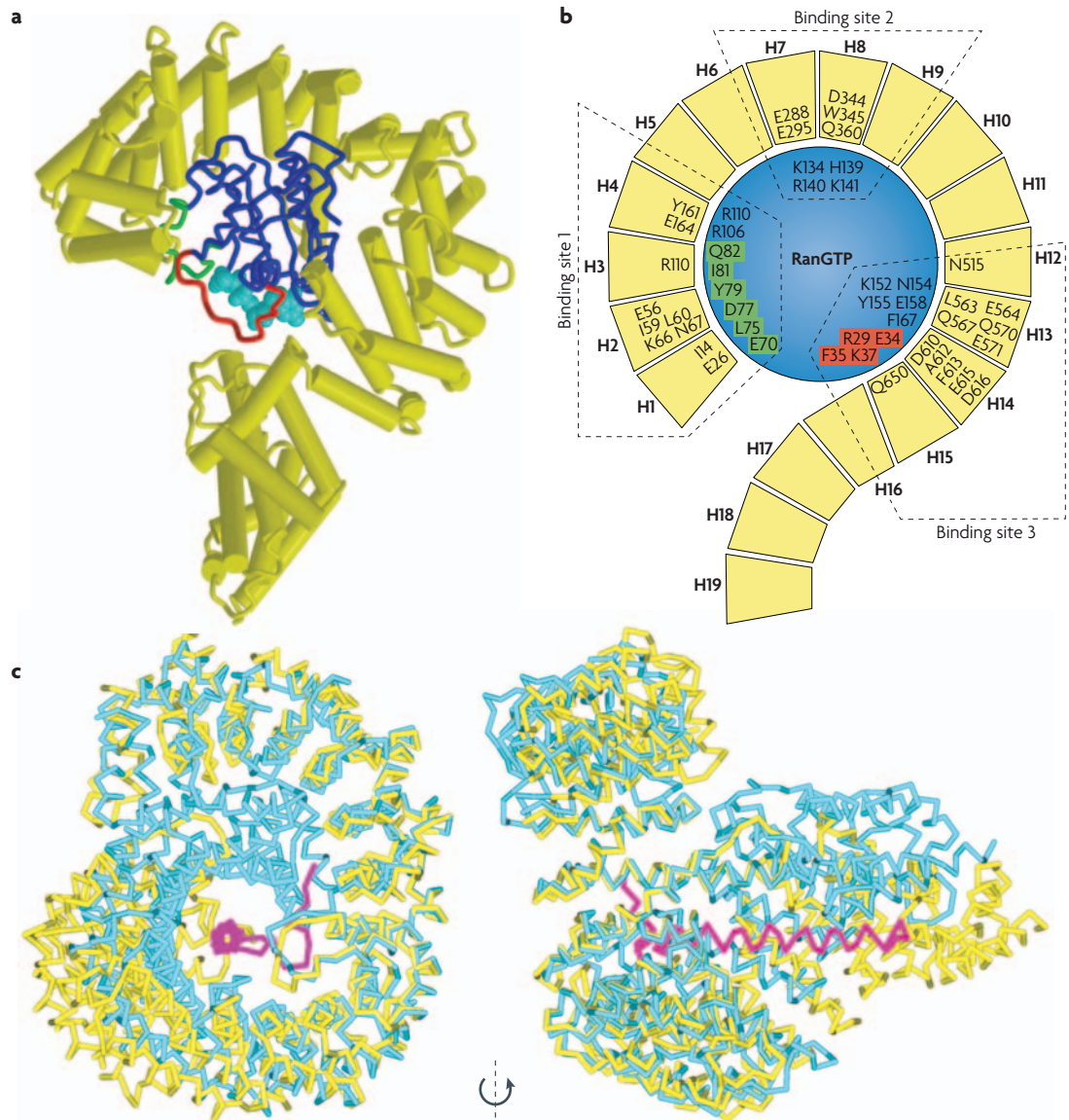


**Figure 3 | Import-complex disassembly.** **a** | Structure of the *Saccharomyces cerevisiae* importin- $\beta$ :RanGTP<sup>74</sup> complex showing how importin- $\beta$  (shown in yellow) coils around Ran (blue). Bound GTP is shown in cyan, whereas the Ran switch I loop is in red and the switch II loop is in green. **b** | Schematic representation of the structure shown in part **a**. The HEAT repeats from which importin- $\beta$  is constructed are shown as yellow blocks (H1–19). The residues that form the interface between importin- $\beta$  (yellow) and RanGTP (blue) are indicated (Ran switch I residues are in red and switch II are in green)<sup>7</sup>. RanGTP binds at three different sites. The first site primarily involves residues in the switch II loop (green) that bind to HEAT repeats 1–4; the second site involves a basic patch on Ran (K134, H139, R140 and K141) that binds electrostatically to acidic residues in HEAT repeats 7 and 8; and the third site primarily involves residues in the switch I loop (red) that interact with HEAT repeats 12–15. The third site is crucial for locking importin- $\beta$  into a conformation in which it cannot bind the importin- $\beta$  binding (IBB) domain of importin- $\alpha$ . **c** | Two views rotated by 90° about the vertical that illustrate the conformational changes in importin- $\beta$  that take place when RanGTP binds to importin- $\beta$ , dissociating the importin- $\alpha$ : $\beta$  complex. The cyan trace shows the conformation of importin- $\beta$  when bound to the IBB domain (magenta trace) in the absence of RanGTP. The yellow trace shows the conformation of importin- $\beta$  when bound to RanGTP. The dramatic conformational change that follows Ran binding disrupts the precise match between the importin- $\beta$  helix and the IBB  $\alpha$ -helix<sup>75</sup>. See also [Supplementary information S4](#) (movie). Parts **a** and **b** of the figure are reproduced with permission from REF. 74 © (2005) Macmillan Magazines Ltd.



In the importin- $\beta$ :IBB-domain complex<sup>74</sup> (BOX 2 and **Supplementary information S2** (movie)), there is extensive electrostatic interaction between the basic IBB domain and acidic residues that form an almost continuous negatively charged patch on the inner surface of importin- $\beta$ . This extensive interaction requires a precise match between the helicoidal pitch of importin- $\beta$  and the  $\alpha$ -helix assumed by the IBB domain, so that importin- $\beta$  coils around the IBB domain. The conformational change in importin- $\beta$  brought about by RanGTP binding disrupts the match between the importin- $\beta$  helicoid and the IBB-domain helix and consequently prevents their interacting efficiently<sup>74</sup> (FIG. 3c and **Supplementary information S4** (movie)).

Importin- $\beta$  is constructed from 19 HEAT repeats (H1–19), each of which is based on two  $\alpha$ -helices (BOX 2; FIG. 3) that stack together to generate an elongated helicoidal molecule<sup>56,74,75</sup>. RanGTP binds to three sites on importin- $\beta$ <sup>73,74</sup> (FIG. 3a,b and **Supplementary information S5** (movie)). The switch II loop binds near the importin- $\beta$  N terminus to a region that encompasses HEAT repeats 1–4 and that is common to all  $\beta$ -karyopherins<sup>76</sup>. A similar switch II loop interaction is observed in complexes of RanGTP with either transportin<sup>77</sup> or CAS<sup>33</sup>. The second Ran-binding site on importin- $\beta$  involves a mainly electrostatic interaction with a loop in HEAT repeat 8 (REFS 73,74). The third RanGTP-binding site involves the switch I loop interacting with HEAT repeats 12–15 and is crucial for generating the conformational change that increases the helicoidal pitch<sup>74</sup>. In the importin- $\beta$ :IBB-domain complex, the path followed by the importin- $\beta$  helicoid would clash with Ran. RanGTP binding can therefore only be accommodated if the importin- $\beta$  chain moves, which in turn generates the increase in helicoidal pitch that releases the IBB domain. An electrostatic interaction between the Lys37 and Lys152 residues of Ran with a cluster of negatively charged residues on importin- $\beta$  is central to this interaction and, although disruption of this interaction with K37D/K152A-Ran does not prevent RanGTP binding to importin- $\beta$ , it does inhibit IBB-domain release<sup>74</sup>.

**Cargo release.** Although dissociation of importin- $\alpha$  from importin- $\beta$  makes import irreversible, it is still necessary to dissociate the cargo from importin- $\alpha$ . When released from importin- $\beta$  by RanGTP, the IBB domain competes with the NLS of the cargo for binding to importin- $\alpha$ , thereby decreasing the affinity of the cargo for importin- $\alpha$  and so facilitating release<sup>32</sup> through an autoinhibitory mechanism (FIG. 2e). An analogous mechanism has been proposed for the release of M9 NLSs from transportin, whereby a loop in HEAT repeat 8 of transportin has been proposed to compete for the NLS-binding site when it is released by RanGTP<sup>18,77</sup>.

Because importin- $\alpha$  has substantial affinity for classic NLSs (generally  $\sim 10$  nM), the off-rate is too slow to accommodate transport rates of  $\sim 100$ – $1,000$  per second per NPC<sup>16</sup>. FG-nucleoporins located at the NPC nuclear face, such as *S. cerevisiae* Nup1 and Nup2, accelerate disassembly<sup>35,36,56,68</sup> of the importin- $\alpha$ : $\beta$ :cargo import complex, and deletion of either nucleoporin produces growth defects.

Nup1 has a higher affinity for the importin- $\alpha$ : $\beta$  import complex than other nucleoporins<sup>56,68</sup> and so concentrates the import complex at the nuclear face of the pore, therefore increasing the rate of binding to RanGTP. Similarly, because it can bind both RanGTP and CAS, the export carrier of importin- $\alpha$ , Nup2, can also increase the rate of import-complex disassembly by increasing the local concentration of these factors<sup>34</sup>. However, Nup2 (and its metazoan counterpart, NUP50) also actively displace both monopartite and bipartite NLSs from importin- $\alpha$  by increasing their off-rate<sup>34,35,68</sup>. Structural studies<sup>34,35</sup> (FIG. 4 and **Supplementary information S6** (movie)) show that Nup2/NUP50 bind importin- $\alpha$  at two sites: a high-affinity site at the importin- $\alpha$  C terminus and a lower affinity site that overlaps the NLS-binding sites. Binding of Nup2/NUP50 to the high-affinity site at the importin- $\alpha$  C terminus greatly increases the local concentration of the domain of Nup2/NUP50 that binds to the lower affinity site and so accelerates the NLS off-rate by a mechanism analogous to that proposed for the IBB domain<sup>32,35</sup>.

#### Step 4: importin recycling

Following import-complex disassembly by RanGTP, the importins have to be recycled to the cytoplasm. Importin- $\beta$  is recycled complexed with RanGTP, whereas importin- $\alpha$  is exported actively by CAS<sup>1–11</sup>. The structure of the *S. cerevisiae* CAS:importin- $\alpha$ :RanGTP export complex (FIG. 5a and **Supplementary information S7** (movie))<sup>33</sup> shows that CAS coils around both RanGTP and importin- $\alpha$  with an unusually large interaction interface. CAS is structurally similar to importin- $\beta$  and is based on 19 HEAT repeats. In the complex, the IBB domain is bound to the importin- $\alpha$  NLS-binding sites, and mutagenesis studies<sup>33</sup> have shown that this binding is crucial for export-complex formation. Therefore, mutations that interfere with the binding of the IBB domain to either the NLS sites or to CAS prevent formation of the export complex. An important consequence of the central role of the IBB domain in the formation of the export complex is that the complex can only form when the cargo has been released from importin- $\alpha$ . This feature prevents futile cycles in which importin- $\alpha$  is returned to the cytoplasm still carrying cargo<sup>33</sup>. However, the IBB domain must also displace the Nup2/NUP50 bound to importin- $\alpha$ , and this is made more difficult by these nucleoporins binding to importin- $\alpha$  with higher affinity than NLSs<sup>35</sup>. It has been proposed<sup>35</sup> that the key to this dilemma is the way in which CAS binds to importin- $\alpha$  (FIG. 5). In the export complex, there would be a steric clash if Nup2/NUP50 remained bound to the importin- $\alpha$  C terminus, and so it seems that Nup2/NUP50 is removed in a two-step mechanism that is the converse of the way in which Nup2/NUP50 displaces NLSs. Therefore, CAS first displaces Nup2/NUP50 from the high-affinity site at the importin- $\alpha$  C terminus, which then facilitates the IBB domain displacing Nup2/NUP50 from the NLS-binding sites, as illustrated in FIG. 5d.

The way in which importin- $\alpha$  interacts first with Nup2/NUP50 and then with CAS ensures the directionality of the cargo-release steps of the cycle and so provides a molecular ratchet to prevent futile cycles<sup>35</sup>. Moreover, once

#### Helicoid

A spiral that is shaped like the shell of a snail such that its radius decreases progressively along its axis.

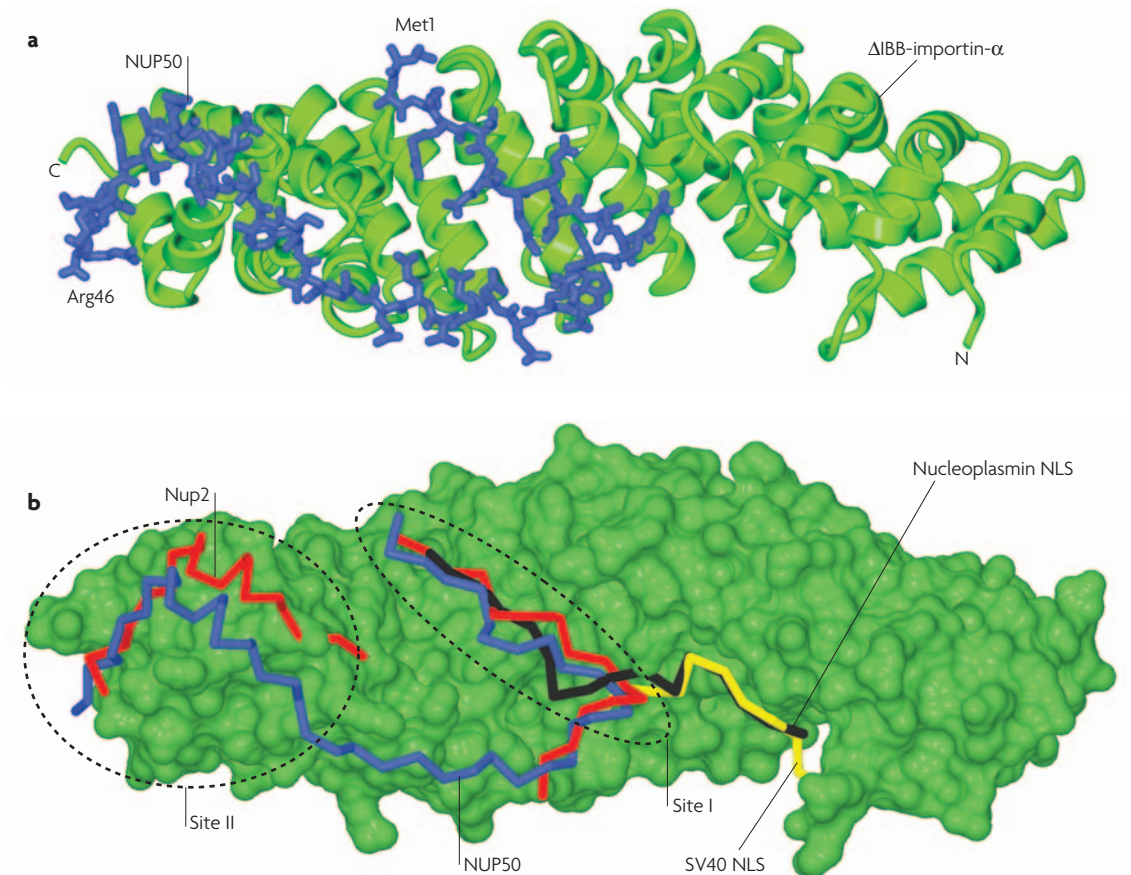


**Figure 4 | Nucleoporin catalysis of import-complex disassembly.** The nucleoporin Nup2 (and its metazoan counterpart, NUP50) binds to two sites on importin- $\alpha$ <sup>34,35</sup>. **a** | Residues 1–46 of NUP50 (blue) bound to importin- $\alpha$  (green). Met1 of NUP50 binds near the middle of importin- $\alpha$ , whereas Arg46 is located near the C terminus of importin- $\alpha$ . **b** | NUP50 (blue) and Nup2 (red) bind to two sites on importin- $\alpha$  (green, space-filling). The strong binding site at the C terminus of importin- $\alpha$  (site II) anchors the nucleoporins to importin- $\alpha$ , whereas the weaker binding site near the midpoint of importin- $\alpha$  (site I) overlaps the nuclear localization signal (NLS)-binding sites and leads to active displacement of bound NLSs (black is nucleoplasmin and yellow is SV40, both of which overlap at the primary NLS-binding site; see FIG. 2). The figure is modified with permission from REF. 35 © (2005) Macmillan Magazines Ltd.

released from importin- $\beta$ , the high local concentration of the IBB domain that results from its physical attachment to importin- $\alpha$  facilitates NLS release<sup>32</sup>. The same principle is observed with Nup2/NUP50 — the high-affinity binding site for Nup2/NUP50 at the importin- $\alpha$  C terminus leads to a high local concentration of the region that displaces NLSs, but is then reversed when CAS displaces the high-affinity Nup2/NUP50-binding region<sup>35</sup>. Although for simplicity all these interactions have been considered as separate steps, it is likely that the series of interactions at the NPC nucleoplasmic face involved in import-complex disassembly and importin recycling occur in a concerted manner with nucleoporins such as Nup1 and Nup2 functioning as scaffolds to coordinate the process.

Once the importin- $\beta$ :RanGTP and CAS:RanGTP:importin- $\alpha$  complexes return to the cytoplasm through the NPCs, cytoplasmic RanGAP (together with the accessory protein RanBP1, which removes RanGTP from importin- $\beta$ <sup>78</sup>) stimulates GTP hydrolysis that releases Ran from importin- $\beta$  and CAS, freeing the importins for another import cycle<sup>1–11</sup>. Although it has not been documented in such detail, it is likely that importin

release and import-complex disassembly might also be coordinated by nucleoporins located on the cytoplasmic face of the NPC (such as RanBP2, which has the potential to bind RanGAP, importin- $\beta$  and Ran), binding the different components and bringing them together in a coordinated manner.

The conformation of the free CAS generated following RanGTP hydrolysis<sup>79</sup> shows a marked change in helicoidal pitch compared with the CAS:importin- $\alpha$ :RanGTP export complex<sup>33</sup> (FIG. 5b and [Supplementary information S7–S9](#) (movies)). When freed of Ran and importin- $\alpha$  in the cytoplasm, CAS takes up a closed conformation in which residues at its N terminus bind to a region near the centre of the molecule<sup>79</sup>. This closed conformation contrasts with the more open conformation adopted in the export complex and is probably rigid, analogous to the more rigid form that importin- $\beta$  assumes when complexed with RanGTP<sup>9</sup>. Certainly the considerable difference in helicoidal pitch seen between the two functional states of CAS is consistent with the molecule having considerable conformational flexibility, similar to that of importin- $\beta$ <sup>9</sup>.

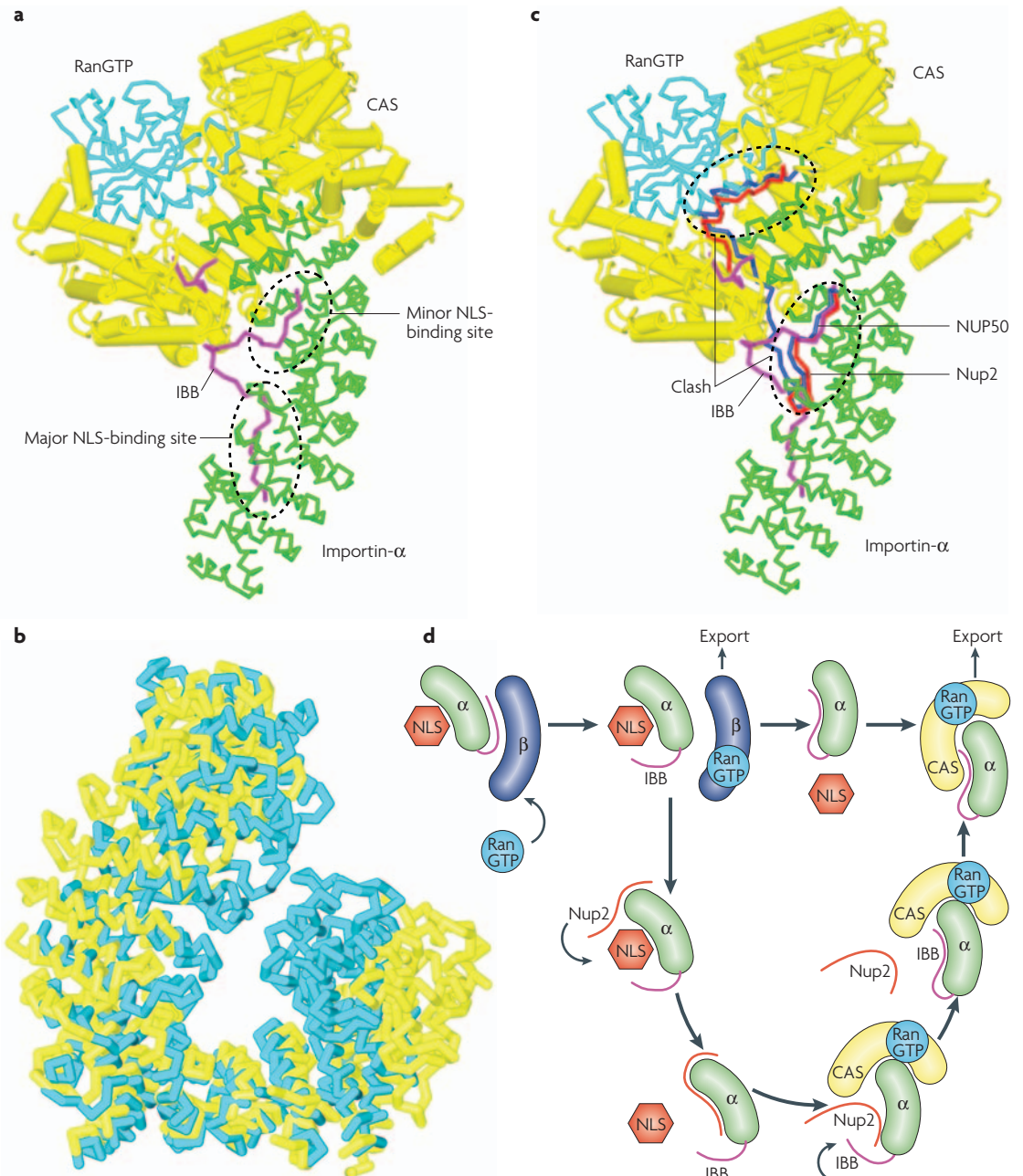


**Figure 5 | Nuclear export of importin- $\alpha$ .** **a** | The structure of the *Saccharomyces cerevisiae* CAS:importin- $\alpha$ :RanGTP export complex<sup>33</sup> shows how the importin- $\beta$  binding (IBB) domain (magenta) is locked against importin- $\alpha$  (green), occupying the same site as that bound by nuclear localization signals (NLSs) (see also FIG. 2e). This interaction is crucial for the formation of the complex and can only occur when cargo has been released. As observed with importin- $\beta$ , CAS (yellow) coils around both importin- $\alpha$  and RanGTP (cyan) in the complex. **b** | Illustration of the substantial conformational change between CAS in the export complex<sup>33</sup> (yellow) and the isolated molecule<sup>79</sup> that is formed after RanGTP hydrolysis in the cytoplasm (cyan) (see also [Supplementary information S9, S10](#) (movies)). **c** | Nup2 (red; and its metazoan counterpart, NUP50 (blue)) binding to the high-affinity site at the C terminus of importin- $\alpha$  would clash with CAS in the export complex. Therefore, CAS first displaces Nup2/NUP50 from the high-affinity site at the C terminus of importin- $\alpha$ , which then facilitates the IBB domain displacing it from the NLS-binding sites. This explains how CAS binding can displace Nup2/NUP50 (REF. 35). **d** | Schematic illustration of the series of interactions in *S. cerevisiae* involving Nup2 (red) and CAS (yellow) that leads to displacement of the NLS and generates a molecular ratchet to prevent futile cycles in which the cargo is returned to the cytoplasm<sup>35</sup>. After NLS is released from importin- $\beta$  by RanGTP (cyan), the IBB domain (magenta) can displace the NLS-containing cargo from importin- $\alpha$ , allowing CAS complexed to RanGTP to bind. This enables recycling of importin- $\alpha$  to the cytoplasm. This process is catalysed by Nup2 that first displaces the NLS and is then itself displaced by CAS. This series of interactions also generates a molecular ratchet to prevent futile transport cycles. Part **a** is modified with permission from REF. 33 © (2004) Macmillan Magazines Ltd. Part **b** is modified from REF. 35 © (2005) Macmillan Magazines Ltd.

### Importance of molecular flexibility

The considerable variation in helicoidal pitch seen with both importin- $\beta$  and CAS in different functional states (FIGS 3, 5 and [Supplementary information S4, S9, S10](#) (movies)) indicates that these molecules are flexible<sup>9,33,74,75,79–81</sup>. The tandem HEAT repeats in importin- $\beta$  and CAS can be thought of as a tightly wound helical spring<sup>81</sup> (BOX 2), such that small changes in the relative orientation of successive HEAT coils could cumulatively generate substantial changes in the helicoidal pitch<sup>33,74</sup>. These local movements could also be combined with hinge-like movements of segments containing several HEAT repeats<sup>9,79</sup>.

Molecular flexibility enables importin- $\beta$  to bind a wide range of different partners through an induced-fit mechanism that involves changes in helicoidal pitch. This can be seen, for example, when comparing the conformations of its complexes with the IBB domain and with RanGTP (FIG. 3c and [Supplementary information S4](#) (movie)). The way in which  $\beta$ -karyopherins coil around their partners implies that the molecules generally do not fit together in a simple recognition interface and, instead, importin- $\beta$  and CAS probably gradually wrap around their cargo. Consequently, flexibility facilitates the formation of cargo:carrier complexes with large intimate interaction interfaces.

The distortion of the helicoids required to wrap around partners has been proposed to store energy that can be used to facilitate complex disassembly<sup>9,33,74</sup>. In this model, energy stored by distorting the helicoid would be counterbalanced by energy liberated by the interaction interface to generate 'spring-loaded' complexes that could dissociate easily following RanGTP hydrolysis. This mechanism would accommodate large interfaces (associated with a high interaction energy, and therefore high specificity) while allowing transitions between states to be achieved using a smaller amount of energy. Such a mechanism might be helpful in facilitating the precise molecular recognition that is a prerequisite for the carefully orchestrated series of interactions needed in nuclear transport cycles.

### Quantitative models of the import cycle

Because the concentrations of the components and their binding constants are known, efforts have been made to develop quantitative models of the nuclear protein import cycle<sup>82–84</sup> or of nuclear export<sup>85</sup>, using methods broadly similar to those used to model metabolic pathways. These models have been useful in identifying several key aspects of the cycle and its orchestration, and have also yielded some unanticipated insights. Although nuclear transport is an active process, it often does not pump against a concentration gradient. Instead, its role is frequently primarily to facilitate the passage of selected molecules between compartments. Therefore, the rate of transport might be more important than the concentration gradient that can be pumped against, and so analogies with other well characterized transport systems, such as the  $K^+/Na^+$ -pump (for which the emphasis is more on equilibrium), might not always be helpful. In nuclear transport, the energy is not used to directly

transport material, but instead is used primarily to recognize the material to be transported and to distinguish between the nucleus and cytoplasm. Therefore, the overall transport rate tends to be determined by the rates of cargo:carrier complex formation in the cytoplasm and dissociation in the nucleus, rather than by the rate of movement through NPCs.

One approach has modelled the RanGTP gradient<sup>82</sup> and has shown that the concentration of nuclear RanGTP is probably ~1,000 times greater than cytoplasmic RanGTP. The kinetics of nuclear protein import was reproduced by a computer model based on known concentrations, rates and binding constants<sup>82</sup>. This model envisaged the fully reversible passage of cargo:carrier complexes through NPCs coupled with RanGTP-induced dissociation of the import complex in the nucleus<sup>82</sup>. However, the on-rate for RanGTP binding to importin- $\beta$  is too slow to account for observed transport rates and so must be accelerated, consistent with the active role identified for FG-nucleoporins on the NPC nucleoplasmic face<sup>34,35,68</sup>.

In another study<sup>83,84</sup>, a systems analysis approach based on a computer simulation coupled with real-time kinetic assays was used to study importin- $\beta$ -mediated import. This model reflected the experimentally determined rates and correctly predicted that import is limited primarily by the concentrations of importin- $\alpha$  and nuclear RanGTP. Increasing the concentration of importin- $\alpha$  increases the rate of import-complex formation, whereas increasing the concentration of nuclear RanGTP increased the rate of import-complex disassembly. Some unexpected predictions of the model, which were verified experimentally, were that increasing the concentration of either importin- $\beta$  or RanGEF inhibits, rather than stimulates, nuclear protein import<sup>83</sup>. This inhibition was caused by changes to the nuclear RanGTP concentration. Sensitivity analysis indicated that probably neither the concentration of CAS nor the permeability of the NPC for cargo:carrier complexes is rate limiting. However, this model was not able to account for the increased rate of nuclear import observed in response to increasing the RanBP1 concentration, and so clearly some aspects of the transport cycle are still not completely understood. Moreover, catalytic steps, such as those involving Nup1 and Nup2, were not included.

### Conclusions

The classic nuclear protein import cycle shows how a spatially and temporally organized series of interactions between macromolecular components can generate a complex biological function. How soluble carriers recognize and release cargoes in the appropriate compartment and how Ran orchestrates these interactions by inducing conformational changes that are facilitated by  $\beta$ -karyopherin flexibility are now well understood. However, more information is still required on the active displacement steps needed to ensure sufficiently rapid dissociation of complexes in both the nucleus and the cytoplasm and on how these steps might be coordinated by nucleoporins. Initial attempts to generate quantitative models of the nuclear protein import cycle have been

#### Sensitivity analysis

A procedure to determine the sensitivity of the outcomes of a model to changes in its parameters.

encouraging, and this approach shows considerable promise for gaining further insight into the molecular mechanisms involved. Moreover, it seems likely that many of the general concepts developed for the classic nuclear protein import cycle can be extended to other nuclear transport cycles, although the details of the molecular recognition steps will be necessarily different and, except for transportin<sup>18</sup>, their precise structural basis still needs to be determined. However, the way in

which some macromolecules are selectively transported through NPCs while others are excluded remains controversial, as does the way in which FG-nucleoporin chains are arranged in the transport channel. Therefore, although great progress has been made in identifying and characterizing the molecular interactions in the soluble phase that drive this nuclear protein import cycle, understanding the precise mechanism of translocation through the NPCs remains an important future challenge.

1. Görlich, D. & Kutay, U. Transport between the cell nucleus and the cytoplasm. *Ann. Rev. Cell Dev. Biol.* **15**, 607–660 (1999).
2. Macara, I. G. Transport into and out of the nucleus. *Microbiol. Mol. Biol. Rev.* **65**, 570–594 (2001).
3. Chook, Y. M. & Blobel, G. Karyopherins and nuclear import. *Curr. Opin. Struct. Biol.* **11**, 703–715 (2001).
4. Conti, E. & Izaurralde, E. Nuclear transport enters the atomic age. *Curr. Opin. Cell Biol.* **13**, 310–319 (2001).
5. Fahrenkrog, B. & Aebi, U. The nuclear pore complex: nucleocytoplasmic transport and beyond. *Nature Rev. Mol. Cell Biol.* **4**, 757–766 (2003).
6. Mosammaparast, N. & Pemberton, L. F. Karyopherins: from nuclear-transport mediators to nuclear-function regulators. *Trends Cell Biol.* **14**, 547–556 (2004).
7. Pemberton, L. F. & Paschal, B. M. Mechanisms of receptor-mediated nuclear import and nuclear export. *Traffic* **6**, 187–198 (2005).
8. Madrid, A. S. & Weis, K. Nuclear transport is becoming crystal clear. *Chromosoma* **115**, 98–109 (2006).
9. Conti, E., Müller, C. W. & Stewart, M. Karyopherin flexibility in nucleocytoplasmic transport. *Curr. Opin. Struct. Biol.* **16**, 237–244 (2006).
10. Stewart, M. *et al.* Molecular mechanism of translocation through nuclear pore complexes during nuclear protein import. *FEBS Lett.* **498**, 145–149 (2001).
11. Weis, K. Regulating access to the genome. Nucleocytoplasmic transport throughout the cell cycle. *Cell* **112**, 441–451 (2003).
12. Feldherr, C. M., Akin, D. & Cohen, R. J. Regulation of functional nuclear pores size in fibroblasts. *J. Cell Sci.* **114**, 4621–4627 (2001).
13. Rout, M. P. & Wente, S. R. Pores for thought: nuclear pore complex proteins. *Trends Cell Biol.* **4**, 357–365 (1994).
14. Rout, M. P. *et al.* The yeast nuclear pore complex: composition, architecture, and transport mechanism. *J. Cell Biol.* **148**, 635–651 (2000).  
**A landmark paper that established the complete protein composition of yeast NPCs together with the location of each nucleoporin as determined by electron microscopy. The authors also proposed an entropic gating mechanism to prevent entry of inappropriate material into the NPC transport channel.**
15. Cronshaw, J. M., Krutchinsky, A. N., Zhang, W., Chait, B. T. & Matunis, M. J. Proteomic analysis of the mammalian nuclear pore complex. *J. Cell Biol.* **158**, 915–927 (2002).
16. Timney, B. L. *et al.* Simple kinetic relationships and nonspecific competition govern nuclear import rates *in vivo*. *J. Cell Biol.* **175**, 579–593 (2006).
17. Mosammaparast, N. *et al.* Nuclear import of histone H2A and H2B is mediated by a network of karyopherins. *J. Cell Biol.* **153**, 251–262 (2001).
18. Lee, B. J. *et al.* Rules for nuclear localization sequence recognition by karyopherin $\beta$ . *Cell* **126**, 543–558 (2006).
19. Ribbeck, K. & Görlich, D. Kinetic analysis of translocation through nuclear pore complexes. *EMBO J.* **20**, 1320–1330 (2001).  
**Presents a careful analysis of nuclear protein import kinetics and proposes a selective phase model based on the formation of a hydrogel formed by interactions between the hydrophobic cores of FG repeats.**
20. Ribbeck, K., Lipowsky, G., Kent, H. M., Stewart, M. & Görlich, D. NTF2 mediates nuclear import of Ran. *EMBO J.* **17**, 6587–6598 (1998).
21. Smith, A. E., Brownawell, A. & Macara, I. G. Nuclear import of Ran is mediated by the transport factor NTF2. *Curr. Biol.* **8**, 1403–1406 (1998).
22. Conti, E., Uy, M., Leighton, L., Blobel, G. & Kuriyan, J. Crystallographic analysis of the recognition of a nuclear localization signal by the nuclear import factor karyopherin- $\alpha$ . *Cell* **94**, 193–204 (1998).  
**Pioneering determination of the structure of yeast importin- $\alpha$  and the way in which it binds NLSs.**
23. Conti, E. & Kuriyan, J. Crystallographic analysis of the specific yet versatile recognition of distinct nuclear localization signals by karyopherin- $\alpha$ . *Structure Fold. Des.* **8**, 329–338 (2000).
24. Fontes, M. R., The, T. & Kobe, B. Structural basis of recognition of monopartite and bipartite nuclear localization sequences by mammalian importin- $\alpha$ . *J. Mol. Biol.* **297**, 1183–1194 (2000).
25. Hodel, M. R., Corbett, A. H. & Hodel, A. E. Dissection of a nuclear localization signal. *J. Biol. Chem.* **276**, 1317–1325 (2001).
26. Catimel, B. *et al.* Biophysical characterization of interactions involving importin- $\alpha$  during nuclear import. *J. Biol. Chem.* **276**, 34189–34198 (2001).
27. Rodriguez, M. *et al.* A cytotoxic ribonuclease variant with a discontinuous nuclear localization signal constituted by basic residues scattered over three areas of the molecule. *J. Mol. Biol.* **360**, 548–557 (2006).
28. Lee, S. J. *et al.* The structure of importin- $\beta$  bound to SREBP-2: nuclear import of a transcription factor. *Science* **302**, 1571–1575 (2003).
29. Cingolani, G., Bednenko, J., Gillespie, M. T. & Gerace, L. Molecular basis for the recognition of a nonclassical nuclear localization signal by importin  $\beta$ . *Mol. Cell* **10**, 1345–1353 (2002).
30. Görlich, D., Henklein, P., Laskey, R. A. & Hartmann, E. A 41 amino acid motif in importin- $\alpha$  confers binding to importin- $\beta$  and hence transit into the nucleus. *EMBO J.* **15**, 1810–1817 (1996).
31. Weis, K., Ryder, U. & Lamond, A. I. The conserved amino-terminal domain of hSRP1  $\alpha$  is essential for nuclear protein import. *EMBO J.* **15**, 1818–1825 (1996).
32. Kobe, B. Autoinhibition by an internal nuclear localization signal revealed by the crystal structure of mammalian importin  $\alpha$ . *Nature Struct. Biol.* **6**, 388–397 (1999).  
**Pioneering structural paper that proposed how the importin- $\alpha$  IBB domain could have an autoinhibitory function that facilitates cargo release in the nucleus.**
33. Matsuura, Y. & Stewart, M. Structural basis for the assembly of a nuclear export complex. *Nature* **432**, 872–877 (2004).  
**Describes the structure of the yeast CAS:RanGTP: importin- $\alpha$  complex, showing the central role of the IBB domain in preventing futile cycles in which cargo is returned to the cytoplasm. Also proposes a spring-loaded model to account for how karyopherin flexibility can mediate the release of importin- $\alpha$  following GTP hydrolysis on Ran.**
34. Matsuura, Y., Lange, A., Harreman, M. T., Corbett, A. H. & Stewart, M. Structural basis for Nup2p function in cargo release and karyopherin recycling in nuclear import. *EMBO J.* **22**, 5358–5369 (2003).
35. Matsuura, Y. & Stewart, M. Nup50/Npap60 function in nuclear protein import complex disassembly and importin recycling. *EMBO J.* **24**, 3681–3689 (2005).  
**Demonstration of active displacement of cargo from importin- $\alpha$  by NUP50 and how this can generate a molecular ratchet to prevent futile cycles.**
36. Goldfarb, D. S., Corbett, A. H., Mason, D. A., Harreman, M. T. & Adam, S. A. Importin  $\alpha$ : a multi-purpose nuclear receptor. *Trends Cell Biol.* **14**, 505–514 (2004).
37. Hodel, H. E. *et al.* Nuclear localization signal-receptor affinity correlates with *in vivo* localization in *S. cerevisiae*. *J. Biol. Chem.* **281**, 23545–23556 (2006).
38. Yang, W., Gelles, J. & Musser, S. M. Imaging of single-molecule translocation through nuclear pore complexes. *Proc. Natl Acad. Sci. USA* **101**, 12887–12892 (2004).  
**Direct demonstration of the random-walk diffusion of import complexes in the central transport channel of NPCs.**
39. Kubitschek, U. *et al.* Nuclear transport of single molecules: dwell times at the nuclear pore complex. *J. Cell Biol.* **168**, 233–243 (2005).
40. Wang, W. & Musser, S. M. Nuclear import time and transport efficiency depend on importin  $\beta$  concentration. *J. Cell Biol.* **174**, 951–961 (2006).
41. Bayliss, R. *et al.* Interaction between NTF2 and xFxFG nucleoporins is required for the nuclear import of RanGDP. *J. Mol. Biol.* **293**, 579–593 (1999).
42. Bayliss, R., Littlewood, T. & Stewart, M. Structural basis for the interaction between FxFG nucleoporin repeats and importin- $\beta$  in nuclear trafficking. *Cell* **102**, 99–108 (2000).  
**Describes the structural basis for the interaction between importin- $\beta$  and FG-nucleoporin cores.**
43. Bayliss, R., Littlewood, T., Strawn, L. A., Wente, S. R. & Stewart, M. GLFG and FxFG nucleoporins bind to overlapping sites on importin- $\beta$ . *J. Biol. Chem.* **277**, 50597–50606 (2002).
44. Bayliss, R. *et al.* Structural basis for the interaction between NTF2 and nucleoporin FxFG repeats. *EMBO J.* **21**, 2843–2853 (2002).
45. Fribourg, S., Braun, I. C., Izaurralde, E. & Conti, E. Structural basis for the recognition of a nucleoporin FG repeat by the NTF2-like domain of the TAP/p15 mRNA nuclear export factor. *Mol. Cell* **8**, 645–656 (2001).
46. Grant, R. P., Neuhaus, D. N. & Stewart, M. Structural basis for the interaction between the Tap/NXF1 UBA domain and FG nucleoporins at 1 Å resolution. *J. Mol. Biol.* **326**, 849–858 (2003).
47. Rexach, M. & Blobel, G. Protein import into nuclei: association and dissociation reactions involving transport substrate, transport factors, and nucleoporins. *Cell* **83**, 683–692 (1995).
48. Ribbeck, K. & Görlich, D. The permeability barrier of nuclear pore complexes appears to operate via hydrophobic exclusion. *EMBO J.* **21**, 2664–2671 (2002).
49. Strawn, L. A., Shen, T. & Wente, S. R. The GLFG regions of Nup116p and Nup100p serve as binding sites for both Kap95p and Mex67p at the nuclear pore complex. *J. Biol. Chem.* **276**, 6445–6452 (2001).
50. Strawn, L. A., Shen, T., Shulga, N., Goldfarb, D. S. & Wente, S. R. Minimal nuclear pore complexes define FG repeat domains essential for transport. *Nature Cell Biol.* **6**, 197–206 (2004).  
**Exploration of the importance of the FG-repeat regions of nucleoporins using an innovative method for deleting these regions in *S. cerevisiae*. Whereas up to half the mass of FG repeats can be deleted using particular groups of nucleoporins, deletion from several selected nucleoporins has a marked effect.**
51. Tran, E. J. & Wente, S. R. Dynamic nuclear pore complexes: life on the edge. *Cell* **125**, 1041–1053 (2006).

52. Grote, M., Kubitschek, U., Reichelt, R. & Peters, R. Mapping of nucleoporins to the centre of the nuclear pore complex by post-embedding immunogold electron microscopy. *J. Cell Sci.* **108**, 2963–2972 (1995).
53. Denning, D. P., Uversky, V., Patel, S. S., Fink, A. L. & Rexach, M. The *Saccharomyces cerevisiae* nucleoporin Nup2p is a natively unfolded protein. *J. Biol. Chem.* **277**, 33447–33455 (2002).
54. Denning, D. P., Patel, S. S., Uversky, V., Fink, A. L. & Rexach, M. Disorder in the nuclear pore complex: the FG repeat regions of nucleoporins are natively unfolded. *Proc. Natl Acad. Sci. USA* **100**, 2450–2455 (2003).
55. Paulillo, S. M. *et al.* Nucleoporin domain topology is linked to transport status of the nuclear pore complex. *J. Mol. Biol.* **351**, 784–798 (2005).
56. Liu, S. M. & Stewart, M. Structural basis for the high-affinity binding of nucleoporin Nup1p to the *Saccharomyces cerevisiae* importin- $\beta$  homologue, Kap95p. *J. Mol. Biol.* **349**, 515–525 (2005).
57. Bednenko, J., Cingolani, G. & Gerace, L. Importin  $\beta$  contains a COOH-terminal nucleoporin binding region important for nuclear transport. *J. Cell Biol.* **162**, 391–401 (2003).
58. Ben-Efraim, I. & Gerace, L. Gradient of increasing affinity of importin- $\beta$  for nucleoporins along the pathway of nuclear import. *J. Cell Biol.* **152**, 411–418 (2001).
59. Pyhtila, B. & Rexach, M. A gradient of affinity for the karyopherin Kap95p along the yeast nuclear pore complex. *J. Biol. Chem.* **278**, 42699–42709 (2003).
60. Zeitler, B. & Weis, K. The FG-repeat asymmetry of the nuclear pore complex is dispensable for bulk nucleocytoplasmic transport *in vivo*. *J. Cell Biol.* **167**, 583–590 (2004).
61. Nachury, M. V. & Weis, K. The direction of transport through the nuclear pore can be inverted. *Proc. Natl Acad. Sci. USA* **96**, 9622–9627 (1999). **Direct demonstration that the directionality of nuclear transport can be reversed by reversing the RanGTP gradient. This work shows conclusively that directionality of transport is driven by the Ran nucleotide state and not by a nucleoporin-affinity gradient for importin- $\beta$ .**
62. Lim, R. Y. *et al.* Flexible phenylalanine-glycine nucleoporins as entropic barriers to nucleocytoplasmic transport. *Proc. Natl Acad. Sci. USA* **103**, 9512–9517 (2006). **This paper uses atomic force microscopy to show that FG-repeats can form molecular brushes when bound to gold particles *in vitro*.**
63. Rout, M. P., Aitchison, J. D., Magnasco, M. O. & Chait, B. T. Virtual gating and nuclear transport: the hole picture. *Trends Cell Biol.* **13**, 622–628 (2003).
64. Tanford, C. *The Physical Chemistry of Macromolecules*. (Wiley, New York, 1961).
65. de Gennes, P. G. Conformations of polymers attached to an interface. *Macromolecules* **13**, 1069–1075 (1980).
66. Frey, S., Richter, R. P. & Görlich, D. FG-rich repeats of nuclear pore proteins form a three-dimensional meshwork with hydrogel-like properties. *Science* **314**, 815–817 (2006).
67. Doi, M. & Edwards, S. F. *The Theory of Polymer Dynamics* (Oxford University Press, Oxford, 1986).
68. Gilchrist, D., Mykytko, B. & Rexach, M. Accelerating the rate of disassembly of karyopherin-cargo complexes. *J. Biol. Chem.* **277**, 18161–18172 (2002).
69. Franke, W. W. Structure, biochemistry and functions of the nuclear envelope. *Internat. Rev. Cytol.* (Suppl. 4), 71–236 (1974).
70. Richardson, W. D., Mills, A. D., Dilworth, S. M., Laskey, R. A. & Dingwall, C. Nuclear protein migration involves two steps: rapid binding at the nuclear envelope followed by slower translocation through nuclear pores. *Cell* **52**, 655–664 (1988).
71. Walther, T. C. *et al.* The cytoplasmic filaments of the nuclear pore complex are dispensable for selective nuclear protein import. *J. Cell Biol.* **158**, 63–77 (2002).
72. Rexach, M. & Blobel, G. Protein import into nuclei: association and dissociation reactions involving transport substrate, transport factors and nucleoporins. *Cell* **83**, 683–692 (1995).
73. Vetter, I. R., Arndt, A., Kutay, U., Görlich, D. & Wittinghofer, A. Structural view of the Ran-importin  $\beta$  interaction at 2.3 Å resolution. *Cell* **97**, 635–646 (1999).
74. Lee, S. J., Matsuura, Y., Liu, S. M. & Stewart, M. Structural basis for nuclear import complex dissociation by RanGTP. *Nature* **435**, 693–696 (2005). **The structure of full-length yeast importin- $\beta$  bound to RanGTP shows how Ran binding alters the pitch of the importin- $\beta$  helix and facilitates release of the importin- $\alpha$  IBB domain.**
75. Cingolani, G., Petosa, C., Weis, K. & Müller, C. W. Structure of importin- $\beta$  bound to the IBB domain of importin- $\alpha$ . *Nature* **399**, 221–229 (1999). **Structure of the IBB:importin- $\beta$  complex showing how the 19 HEAT repeats of importin- $\beta$  are arranged to form a helical molecule that coils around the  $\alpha$ -helical IBB domain. Comparison between different crystal forms indicated that importin- $\beta$  might be flexible.**
76. Görlich, D. *et al.* A novel class of RanGTP binding proteins. *J. Cell Biol.* **138**, 65–80 (1997).
77. Chook, Y. M. & Blobel, G. Structure of the nuclear transport complex karyopherin- $\beta$ 2–Ran x GppNHp. *Nature* **399**, 230–237 (1999).
78. Bischoff, F. R. & Görlich, D. RanBP1 is crucial for the release of RanGTP from importin- $\beta$ -related nuclear transport factors. *FEBS Lett.* **419**, 249–254 (1997).
79. Cook, A. *et al.* The structure of the nuclear export receptor Cse1 in its cytosolic state reveals a closed conformation incompatible with cargo binding. *Mol. Cell* **18**, 355–367 (2005). **Direct demonstration of the dramatic conformational change in the yeast homologue of CAS, Cse1. In the absence of RanGTP and importin- $\alpha$ , the Cse1 helix adopts a closed conformation in which the N terminus becomes bound to a region near the centre of the molecule.**
80. Fukuhara, N., Fernandez, E., Ebert, J., Conti, E. & Svergun, D. Conformational variability of nucleocytoplasmic transport factors. *J. Biol. Chem.* **279**, 2176–2181 (2004). **Low-angle X-ray scattering is used to show that several  $\beta$ -karyopherins can adopt different structures in solution, leading to the concept of these molecules having flexible structures.**
81. Stewart, M. Molecular recognition in nuclear trafficking. *Science* **302**, 1513–1514 (2003).
82. Görlich, D., Seewald, M. J. & Ribbeck, K. Characterization of Ran-driven cargo transport and the RanGTPase system by kinetic measurements and computer simulation. *EMBO J.* **22**, 1088–1100 (2003).
83. Riddick, G. & Macara, I. G. A systems analysis of importin- $\alpha$ : $\beta$  mediated nuclear protein import. *J. Cell Biol.* **168**, 1027–1038 (2005). **A comprehensive simulation of the classic nuclear protein import cycle that gives several novel and unanticipated functional insights.**
84. Smith, A., Slepchenko, B. M., Schaff, J. C. Loew, L. M. & Macara, I. G. Systems analysis of Ran transport. *Science* **295**, 488–491 (2002).
85. Becskei, A. & Mattaj, I. W. Quantitative models of nuclear transport. *Curr. Opin. Cell Biol.* **17**, 27–34 (2005).
86. Akey, C. W. Structural plasticity of the nuclear pore complex. *J. Mol. Biol.* **248**, 273–293 (1995).
87. Akey, C. W. & Radermacher, M. Architecture of the *Xenopus* nuclear pore complex revealed by three-dimensional cryo-electron microscopy. *J. Cell Biol.* **122**, 1–19 (1993).
88. Stoffer, D. *et al.* Cryo-electron microscopy provides novel insights into nuclear pore architecture: implications for nucleocytoplasmic transport. *J. Mol. Biol.* **328**, 119–130 (2003). **Comprehensive analysis of NPC morphology using cryo-EM and tomography.**
89. Lim, R. Y. H. & Fahrenkrog, B. The nuclear pore complex up close. *Curr. Opin. Cell Biol.* **18**, 342–347 (2006).
90. Lim, R. Y., Aebi U. & Stoffer, D. From the trap to the basket: getting to the bottom of the nuclear pore complex. *Chromosoma* **115**, 15–26 (2006).
91. Beck, M. *et al.* Nuclear pore complex structure and dynamics revealed by cryoelectron tomography. *Science* **306**, 1387–1390 (2004).
92. Fahrenkrog, B. *et al.* Domain-specific antibodies reveal multiple-site topology of Nup153 within the nuclear pore complex. *J. Struct. Biol.* **140**, 254–267 (2002).
93. Devos, D. *et al.* Components of coated vesicles and nuclear pore complexes share a common molecular architecture. *PLoS Biol.* **2**, e380 (2004).
94. Vetter, I. R., Nowak, C., Nishimoto, T., Kuhlmann, J. & Wittinghofer, A. Structure of a Ran-binding domain complexed with Ran bound to a GTP analogue: implications for nuclear transport. *Nature* **398**, 39–46 (1999).
95. Stewart, M., Kent, H. M. & McCoy, A. J. Structural basis for molecular recognition between nuclear transport factor 2 (NTF2) and the GDP-bound form of the Ras-family GTPase, Ran. *J. Mol. Biol.* **277**, 635–646 (1998).
96. Bullock, T. L., Clarkson, W. D., Kent, H. M. & Stewart, M. The 1.6 Å resolution crystal structure of nuclear transport factor 2 (NTF2). *J. Mol. Biol.* **260**, 422–431 (1996).
97. Renault, L., Kuhlmann, J., Henkel, A. & Wittinghofer, A. Structural basis for guanine nucleotide exchange on ran by the regulator of chromosome condensation (RCC1). *Cell* **105**, 245–255 (2001).
98. Hillig, R. C. *et al.* The crystal structure of rna1p: a new fold for a GTPase activating protein. *Mol. Cell* **3**, 781–791 (1999).
99. Seewald, M. J., Korner, C., Wittinghofer, A. & Vetter, I. R. RanGAP mediates GTP hydrolysis without an arginine finger. *Nature* **415**, 662–666 (2002).

## Competing interests statement

The author declares no competing financial interests.

## DATABASES

The following terms in this article are linked online to UniProtKB: <http://ca.expasy.org/sprot>  
NTF2 | Nup1 | Nup2 | NUP50 | Nup100 | Nup116 | SREBP2

## FURTHER INFORMATION

Murray Stewart's homepage:  
[http://www2.mrc-lmb.cam.ac.uk/SS/Stewart\\_M/group](http://www2.mrc-lmb.cam.ac.uk/SS/Stewart_M/group)  
Access to this links box is available online.

## SUPPLEMENTARY INFORMATION

See online article: S1 (movie) | S2 (movie) | S3 (movie) | S4 (movie) | S5 (movie) | S6 (movie) | S7 (movie) | S8 (movie) | S9 (movie) | S10 (movie) | S11 (movie) | S12 (movie) | S13 (movie) | S14 (movie)  
Access to this links box is available online.